Non-reciprocal electromagnetic metasurface based on the nonlinearity of a liquid metamaterial

Alexander Zharov, Vanessa Fierro, Alain Celzard

Non-reciprocal electromagnetic metasurface based on the nonlinearity of a liquid metamaterial

ALEXANDER ZHAROV[1,*], VANESSA FIERRO[1], AND ALAIN CELZARD[1,†]

[1] Université de Lorraine, CNRS, IJL,F-88000 Epinal, France
[*] alexander.zharov@univ-lorraine.fr
[†] alain.celzard@univ-lorraine.fr

Compiled November 8, 2023

In this paper, we propose the design of a non-reciprocal electromagnetic metasurface, which uses a highly nonlinear liquid metamaterial as a source of non-reciprocity. We show that the proposed metasurface, whose thickness is comparable to the wavelength, can exhibit a difference between the transmission coefficients in the forward and backward directions of up to 0.95. Moreover, the particularly high nonlinearity of the liquid metamaterial enables the radiation power required to induce the nonlinear effects to be considerably reduced compared with natural materials. The feasibility of the proposed metasurface has been verified by numerical simulations.

http://dx.doi.org/10.1364/ao.XX.XXXXXX

In recent years, metasurfaces (MSs) have attracted immense interest from the research community, moving from theoretical concepts to well-developed industrial production [1, 2]. Electromagnetic MSs are typically composed of an array of resonant subwavelength elements arranged in a specific pattern. By carefully designing these elements and their layout, MSs can be tailored to perform a wide range of functions, including focusing light, orienting beams, and even creating holograms [3–5]. As a result, MSs have a number of potential applications in fields such as optics, telecommunications, and sensing, and are an active area of research in both academia and industry [6, 7].

One of the current problems in modern electromagnetics is the development of non-reciprocal optical elements, as this is crucial to the creation of devices such as optical isolators [8]. Non-reciprocity refers to the property of a system in which the response to an input signal is different depending on the direction of this signal. In other words, the system is not symmetric under time reversal transformation. This condition significantly limits the number of possible ways of achieving non-reciprocity. One such method is based on the nonlinear optical response of a material to electromagnetic excitation [9–12]. However, in general, optical nonlinearity is relatively low, requiring extremely high light intensities to produce the desired effect. To increase the nonlinear response, metamaterials can be used [13–15].

In general, a metamaterial is a material designed to have properties not found in natural materials. These properties arise from the way the material is structured at the nanoscale, rather than from the properties of its constituent parts [16]. One particular type of metamaterials, called liquid metamaterials (LMMs), has received a great deal of interest because of its high potential for tunability and reconfigurability [17].

LMMs are a type of artificial material that can exhibit unique and highly tunable mechanical, optical, and electromagnetic properties [18–23]. An example of an LMM is a colloidal suspension, i.e., a liquid containing small particles that can be manipulated by electric or magnetic fields. The ability of these particles to move and regroup under the action of electromagnetic field makes such an LMM a highly nonlinear medium. In this Letter, we propose the design of a non-reciprocal MS using the exceptionally high nonlinearity of an LMM.

The proposed MS consists of a two-dimensional square lattice of identical dielectric resonatorsas schematically shown in Fig. 1. The unit cell contains a dielectric cylinder composed of two layers with different dielectric permittivities immersed in an LMM. The LMM is considered a highly nonlinear medium, whose mechanism of nonlinearity will be discussed further in the text. The cylinders are installed on a substrate whose origin is irrelevant. For calculation purposes, its refractive index has been set to 1.2, as such a low refractive index does not require additional layers and allows simpler and more comprehensible visualizations to be presented. However, the substrate material can be arbitrary, but for higher-refractive-index materials, an additional dielectric layer is desirable to avoid excessive reflection.

The appearance of non-reciprocity can be understood within the framework of a simplistic model. First, let us consider a purely linear problem involving the interaction of a dielectric cylinder with an electromagnetic wave. Down to the lowest order, the electromagnetic response of the cylinder can be approximated as the excitation of electric and magnetic dipole modes. Consider a plane electromagnetic wave incident normal to the MS. In general, the excited electric and magnetic dipole moments can then be written as follows [24]:

$$\mathbf{p} = \hat{\alpha}_e \mathbf{E} + \hat{\alpha}_{em} \mathbf{H}; \quad \mathbf{m} = \hat{\alpha}_{me} \mathbf{E} + \hat{\alpha}_m \mathbf{H}, \tag{1}$$

where $\mathbf{p}$ and $\mathbf{m}$ are the electric and magnetic dipole moments, $\mathbf{E}$ and $\mathbf{H}$ are the local electric and magnetic fields, $\hat{\alpha}_e$ and $\hat{\alpha}_m$ are the electric and magnetic polarizability tensors, and $\hat{\alpha}_{em}$ and $\hat{\alpha}_{me}$ represent the magneto-electric couplings, respectively. Taking into account the isotropy of the cylinders in the xy-plane and the relations between electric and magnetic fields in a plane wave, and assuming x-polarization of the plane wave, one can obtain the expressions for the dipole moments:

$$p_x = \left(\alpha_e^{xx} \pm Z_0^{-1} \alpha_{em}^{xy}\right) E_x; \quad m_y = \left(\pm Z_0^{-1} \alpha_m^{yy} - \alpha_{em}^{xy}\right) E_x, \tag{2}$$

where "$\pm$" represents the forward (along the z-axis) and backward (opposite to the z-axis) propagation directions of the plane wave, respectively, and Z_0 is the impedance of the surrounding medium. In

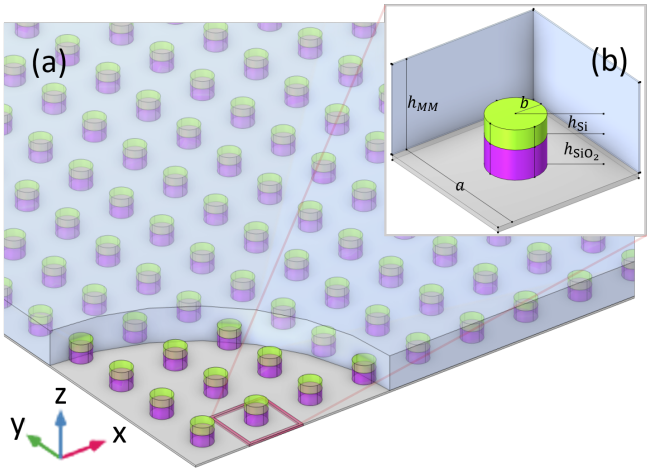

Fig. 1. Schematic view of the proposed MS (a). It consists of a square lattice of dual-layer cylinders immersed in an LMM (blue). Each cylinder has a silicon layer (green) and a silica layer (purple). The inset (b) shows the unit cell of the MS with its primary parameters.

Eq.(2), we took into account that $\alpha_{me}^{yx} = -\alpha_{em}^{xy}$ due to the reciprocity of the medium in the linear regime [24]. Finally, the absolute values of the dipole moments can be calculated as follows:

$$|p_x|^2 = \left(|\alpha_e^{xx}|^2 + \left|Z_0^{-1}\alpha_{em}^{xy}\right|^2 \pm 2Z_0^{-1}\mathrm{Re}\left(\alpha_e^{xx}\alpha_{em}^{xy*}\right)\right)|E_x|^2, \quad (3)$$

$$|m_y|^2 = \left(\left|Z_0^{-1}\alpha_m^{yy}\right|^2 + |\alpha_{em}^{xy}|^2 \mp 2Z_0^{-1}\mathrm{Re}\left(\alpha_m^{yy}\alpha_{em}^{xy*}\right)\right)|E_x|^2, \quad (4)$$

where the asterisk corresponds to complex conjugation. For a homogeneous dielectric cylinder, the cross-term $\mathrm{Re}\left(\alpha_e^{xx}\alpha_{em}^{xy*}\right)$ vanishes due to the absence of magneto-electric coupling, $\hat{\alpha}_{em} = 0$. Therefore, the excitation of the magnetic and electric dipole moments in a homogeneous cylinder is independent of the direction of light propagation. At the same time, the asymmetry of the cylinder with respect to the direction of wave propagation gives rise to spatial dispersion, which leads to the appearance of magneto-electric coupling [12]. In our case, the asymmetry is brought in by the difference in the dielectric constants of the two layers constituting the cylinders. As a result, the excitation of the dipole modes becomes asymmetric with respect to the light propagation direction. It should be noted that, despite the asymmetric dipole excitation, the total scattering does not depend on the propagation direction, thus preserving reciprocity in the linear regime.

The asymmetric dipole excitation results in different near-field distributions for forward and backward illumination. In particular, the near-field distribution produced by an electric dipole moment can be expressed as $\mathbf{E}(\mathbf{r}) = (3(\mathbf{p}\cdot\mathbf{r})\mathbf{r} - r^2\mathbf{p})r^{-5}$, where $\mathbf{r}$ represents the vector connecting the dipole to the observation point and r is the absolute value of vector $\mathbf{r}$. Evidently, the near-field amplitude is proportional to the absolute value of the electric dipole moment. As a result, a large difference between the amplitudes of electric dipoles excited by an electromagnetic wave propagating forwards or backwards leads to a large difference in the amplitudes of the electric field near the dipoles.

On the other hand, when nonlinearity comes into play, the scattering changes drastically. Let us assume for the moment that the nonlinearity is local. In this case, the dielectric permittivity can be expressed as a function of electric field, $\varepsilon(r) = \varepsilon\left(|E(r)|^2\right)$. As a result, the difference in electric field distribution causes the difference in nonlinear permittivity distribution, thus modifying the scattering. In other words, forward- and backward-propagating waves induce different distributions of nonlinear permittivity, which can lead to reciprocity violation.

As the non-reciprocity of the proposed MS relies solely on the nonlinearity of the LMM, it is necessary to give its theoretical description. The origin of this nonlinearity is due to the rearrangement of the structural elements of the LMM under the action of an electromagnetic field, which leads to the appearance of field-dependent, non-uniform effective permittivity. We presume that the LMM under consideration here is formed by a suspension of identical polarizable nanospheres, called meta-atoms, in a viscous liquid. The size of each sphere is assumed much smaller than any other scale of the problem, including the wavelength of the electromagnetic radiation. In addition, we assume that the concentration of the meta-atoms is such that their number in the field inhomogeneity scale is much larger than 1. Thus, the suspension can be treated as a continuous medium whose effective permittivity depends on the volume fraction of nanospheres. For relatively low volume fractions of meta-atoms, the effective permittivity $\varepsilon_{\mathrm{eff}}$ can be approximated by the Maxwell Garnett formula:

$$\varepsilon_{\mathrm{eff}} = \varepsilon_0\varepsilon_h\left(1 + 3\nu\frac{\varepsilon_{MA} - \varepsilon_h}{\varepsilon_{MA}(1-\nu) + \varepsilon_h(2+\nu)}\right), \quad (5)$$

where ε_0 is the permittivity of vacuum, ε_h and ε_{MA} are the relative permittivities of the host medium and meta-atom material, respectively, and $\nu = nV_0$ is the volume fraction of meta-atoms, where n is the meta-atom concentration and V_0 is the volume of a single meta-atom.

In the absence of an external field, the distribution of meta-atoms in thermal equilibrium is spatially uniform. At the same time, in the presence of an inhomogeneous electromagnetic field, the meta-atoms undergo the action of a ponderomotive force that leads to their rearrangement. As a result, the concentration of meta-atoms becomes coordinate-dependent. The distribution of meta-atoms in the presence of an inhomogeneous electromagnetic field can be calculated by applying the equilibrium condition such that the ponderomotive force is counterbalanced by the pressure gradient force, making the average current of the meta-atoms zero (see [15] and references therein):

$$\mathbf{j} = n\mu(\mathbf{f}_{em} + \mathbf{f}_p) = 0, \quad (6)$$

where μ is the particle mobility, $\mathbf{f}_{em}$ is the electromagnetic force, and $\mathbf{f}_p$ is the pressure gradient force. The electromagnetic ponderomotive force can be calculated as follows:

$$\mathbf{f}_{em} = \frac{\alpha}{4}\nabla|E|^2, \quad (7)$$

where $\alpha = 3V_0\varepsilon_0\varepsilon_h\left(\frac{\varepsilon_{MA}-\varepsilon_h}{\varepsilon_{MA}+2\varepsilon_h}\right)$ is the polarizability of a meta-atom. To find the pressure gradient force, we assume that the meta-atom suspension can be treated as a hard-sphere fluid governed by the Carnahan-Starling equation of state [25]: $P = nk_BT\chi(\nu)$, where P is the pressure, k_B is the Boltzmann constant, T is the temperature, and $\chi(\nu) = \left(1 + \nu + \nu^2 - \nu^3\right)/(1-\nu)^2$ is the compressibility factor. The Carnahan-Starling equation is applicable for volume fractions up to ν 0.55 [25]. Thus, the pressure gradient force can be expressed as:

$$\mathbf{f}_p = -\frac{k_BT}{n}\nabla(n\chi(\nu)). \quad (8)$$

Combining Eqs. (6), (7), and (8), an analytical solution relating field intensity and meta-atom filling fraction can be obtained:

$$\frac{\alpha}{4k_BT}|E|^2 = g(\nu) - g(\nu_0), \quad (9)$$

where $g(\nu) = (3-\nu)/(1-\nu)^3 + \log\nu$ and ν_0 is the unperturbed filling fraction. Equation (9) cannot be solved analytically with respect

to the filling fraction, but it provides an unambiguous correspondence between intensity and filling fraction. Hence, Eq. (9) together with Eq. (5) allow the nonlinear effective permittivity of the LMM to be calculated.

In the case of relatively low field intensity, *i.e.*, $\frac{\alpha}{4k_BT}|E|^2 \ll 1$, Eq. (9) can be simplified and solved analytically:

$$\nu \approx \nu_0 \exp\left(\frac{\alpha}{4k_BT}|E|^2\right) \approx \nu_0\left(1+\frac{\alpha}{4k_BT}|E|^2\right). \quad \textbf{(10)}$$

Consequently, an approximate expression for the nonlinear permittivity of the LMM can be obtained by substituting Eq. (10) into Eq. (5):

$$\varepsilon_{\text{eff}}\left(|E|^2\right) \approx \varepsilon_0\varepsilon_h\left(1+3\nu_0\frac{\varepsilon_{MA}-\varepsilon_h}{\varepsilon_{MA}+2\varepsilon_h}\left(1+\frac{\alpha}{4k_BT}|E|^2\right)\right). \quad \textbf{(11)}$$

Certainly, the simplistic model considered here cannot be applied directly to the real world, as the finite-sized cylinder cannot be regarded as a point dipole, the actual electromagnetic mode of the cylinder is generally not a dipole mode, the nonlinearity cannot be treated as local, and the overall scattering problem must be solved self-consistently. However, the calculations can be performed numerically.

Full-wave simulations were performed using COMSOL Multiphysics with RF frequency domain solver. The MS was modeled as a periodic structure with a primitive cell supplemented by periodic boundary conditions. The primitive cell contained one dielectric cylinder composed of two layers, namely a silicon layer and a silicon dioxide layer (see again Fig. 1). The dielectric parameters of silicon and silicon dioxide were obtained from the refractive index database[26]. The dielectric cylinder was immersed in an LMM, treated as an aqueous suspension of 10-nm gold nanospheres. The permittivity of the nanospheres was approximated by the Drude model[27], and the dielectric parameters of water were also obtained from the refractive index database[26]. The effective nonlinear permittivity of the LMM was calculated using Eqs. (5) and (9). Additionally, the permittivity was constrained by the conservation of the total number of meta-atoms, such that $(V_0/V)\int_V n(\mathbf{r})d^3\mathbf{r} = \nu_0$, where V is the volume filled by the LMM. The MS was then illuminated by a plane electromagnetic wave of a given frequency incident normally to the MS in the forward and backward directions. Finally, the transmission coefficients were calculated. The parameters of the primitive cell were optimized using a combination of Monte-Carlo and gradient descend methods. The details of the optimization are presented in the Supplement 1.

Figure 2 shows the simulation results for one of the optimized combinations of parameters. It can be seen that forward propagation has a transmission coefficient above 0.9, while backward propagation is strongly blocked with a transmission coefficient below 0.1. The sharp contrast between forward and backward transmissions takes place in a narrow frequency region of several THz. Figures 2 (c) and (d) show the distribution of the volume fraction in the LMM.

Figure 3 shows the simulation results for another optimized parameter combination. Unlike the previous example, in this case transmission in the forward direction is almost completely suppressed, while backward transmission reaches 0.8. Once again, the high contrast between transmission coefficients for forward and backward propagation directions lies within a relatively narrow frequency range.

Figure 4 shows the multipole decomposition of the modes excited in linear regime in the systems shown in Figs. 2 and 3, which will be further referred to as System 1 and System 2, respectively. Firstly, it is evident that the excited modes differ significantly from purely dipolar excitations. Moreover, while the excitations in System 1 are predominantly dipolar, the excitations in System 2 show a much richer multipole composition. This can be explained by the fact that the cylinder radius in System 2 is larger with respect to the wavelength.

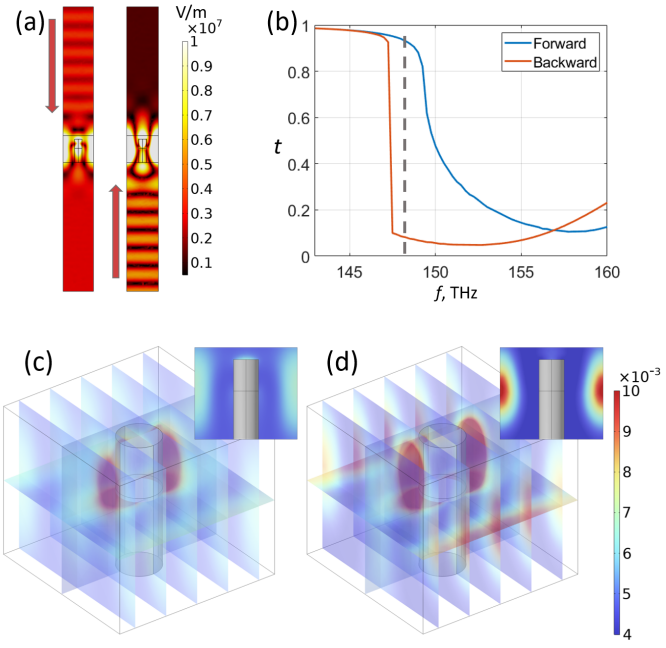

Fig. 2. Example of unidirectional transmission. (a) Electric field distributions for forward and backward propagation. (b) Frequency dependencies of transmission coefficients for forward and backward propagation. (c,d) Distributions of the filling fraction of the LMM meta-atoms for forward propagation (c) and backward propagation (d). The parameters of the MS are as follows: lattice period $a = 1710$ nm; dielectric cylinder radius $b = 210$ nm; silicon thickness $h_{\text{Si}} = 520$ nm; silica thickness $h_{\text{SiO}_2} = 800$ nm; and LMM thickness $h_{MM} = 1520$ nm.

Secondly, the decomposition confirms the hypothesis that the asymmetry in the excitation of multipoles is responsible for the non-reciprocal transmission in the presence of nonlinearity. It is clearly visible that the partial multipole cross-section can differ significantly for forward and backward illumination. It should be noted, however, that the total extinction cross-section does not depend on the direction of illumination in the linear regime.

The proposed nanostructures can be prepared using common nanofabrication techniques. First, the silicon and silicon oxide layers can be formed by chemical vapor deposition. Then, the lattice structure can be shaped by electron-beam lithography using a proper resist and mask. Finally, the structure can be completed using ion etching followed by mask removal. The LMM can then be added on the MS.

The class of systems under consideration may be interesting in several aspects. Firstly, it enables strong optical non-reciprocity in a very thin layer. Indeed, the thickness of the simulated MSs was between 1.5 and 2.5 μm, which is comparable to the wavelength of the incident radiation. Moreover, even with such a small thickness, the system under consideration demonstrated a difference between the transmission coefficients in two opposite directions of up to 0.95. Thanks to optimization, the proposed MS can be tuned to provide optical isolation at a given frequency, which makes it highly adaptable.

On the other hand, the use of a LMM allows a reduction in the radiation power needed to give rise to the nonlinearity. Indeed, optical isolation in the proposed system can be achieved at a power density of 10 kW/cm^2 (see Fig. 5), while to induce sufficient nonlinear effects in natural materials, the necessary values of power density can easily reach GW/cm^2 and more. Such a significant reduction in power density

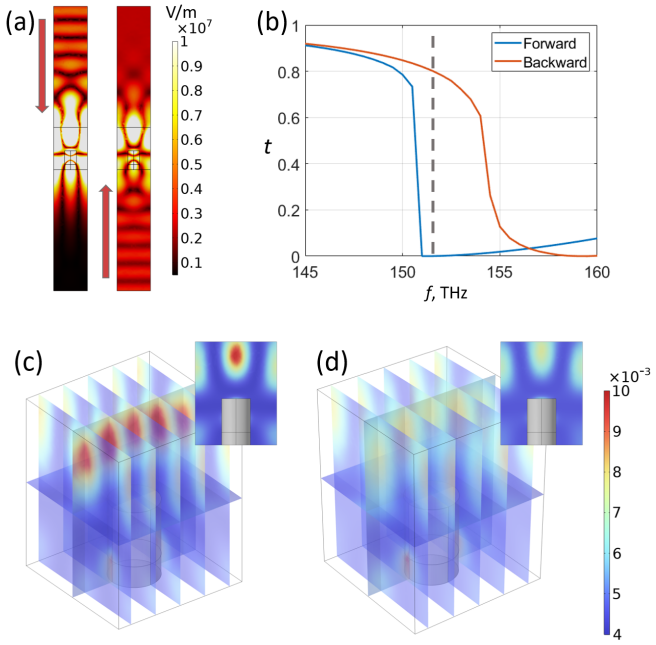

Fig. 3. Same as Fig. 2, but with the following parameters: lattice period $a = 1890$ nm; dielectric cylinder radius $b = 330$ nm; silicon thickness $h_{\mathrm{Si}} = 770$ nm; silica thickness $h_{\mathrm{SiO_2}} = 300$ nm; and LMM thickness $h_{MM} = 2380$ nm.

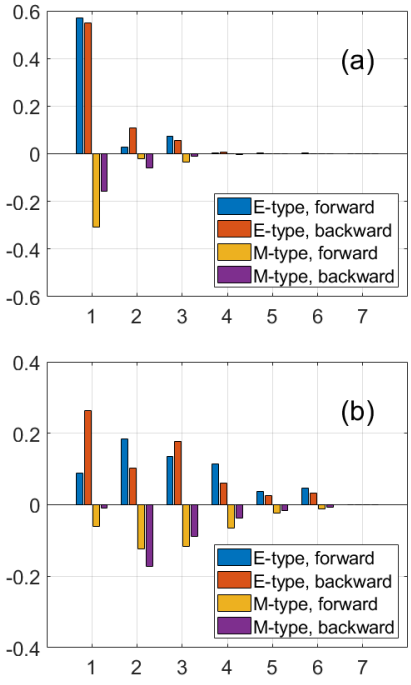

Fig. 4. Multipole decomposition of the electromagnetic modes excited in System 1 (a) and System 2 (b). The partial multipole cross-sections are normalized with respect to the total extinction cross-section, such that the sum of all partial cross-sections is equal to 1. The x-axis represents the order of the multipole: 1 corresponds to dipole, 2 – to quadrupole, 3 – to octupole, *etc*.

results from the peculiar properties of the LMM.

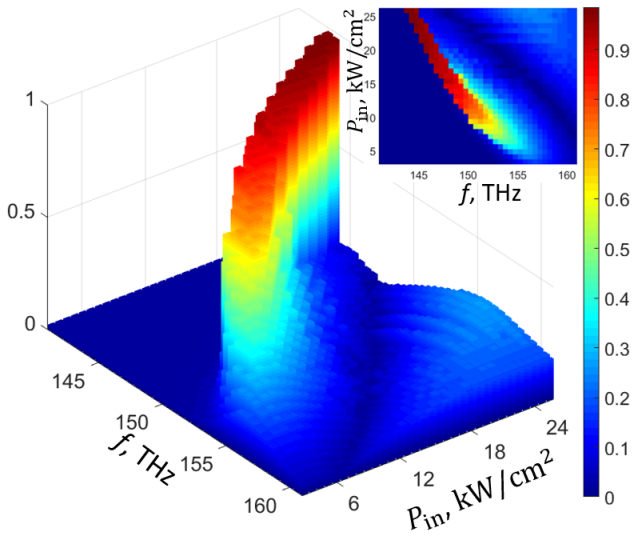

Fig. 5. Absolute value of the difference between forward and backward transmissions as a function of radiation frequency and radiation power for the MS with parameters similar to those in Fig. 2.

Nevertheless, the proposed design is not free from shortcomings. Firstly, the efficient optical isolation only occurs in a narrow frequency range. This is because the non-reciprocal transmission is directly related to the excitation of an eigenmode of a dielectric cylinder, which has its own resonance width. Moreover, the actual non-reciprocal transmission region turns out to be narrower than the resonance width of the dielectric cylinder, as the sufficient asymmetry of the excited mode with respect to the direction of light propagation takes place in a narrow frequency region within the resonance width. As a result, the proposed MS is not suitable for wide frequency range applications.

Secondly, the non-linearity of a LMM is very slow compared to any characteristic time of electromagnetic radiation. The non-linearity under consideration is indeed induced by a physical displacement of particles in a liquid, which requires time. Thus, the proposed system is inapplicable in fields requiring fast switching.

Finally, any non-reciprocal device based on nonlinearity has fundamental limitations. For instance, such devices cannot operate under two or more excitation signals [28].

In conclusion, this paper presents a non-reciprocal MS design using an LMM with high nonlinearity. The proposed MS, consisting of a two-dimensional lattice of dielectric resonators immersed in an LMM, exhibits significant non-reciprocity in its scattering properties. Through theoretical analysis and numerical simulations, it is demonstrated that the non-reciprocity of the proposed MS arises from the asymmetric near-field distributions for forward and backward illumination.

Despite the drawbacks of the proposed MS, such as the slowness of the nonlinearity and the narrow frequency range of the optical isolation, the presented design is promising for various applications, such as isolators or asymmetric power limiters, where a non-reciprocal electromagnetic response is essential. The use of an LMM gives access to extremely high nonlinearity, enabling a significant reduction in the radiation power required to induce nonlinear effects, including non-reciprocal transmission. Future research can explore further optimizations, alternative MS geometries, and the potential for integration with other functional elements to improve the overall performance.

Funding. This study was supported by the French PIA project "Lorraine Université d'Excellence," Reference No. ANR-15-IDEX-04-LUE, and the TALiSMAN and TALiSMAN2 project, funded by ERDF (Grant No. 2019-000214).

Disclosures. The authors declare no conflicts of interest.

Supplemental document. See Supplement 1 for supporting content.

REFERENCES

1. H.-T. Chen, A. J. Taylor, and N. Yu, Reports on Prog. Phys. **79**, 076401 (2016).
2. S. Kruk and Y. Kivshar, ACS Photonics **4**, 2638 (2017).
3. C. L. Holloway, E. F. Kuester, J. A. Gordon, J. O'Hara, J. Booth, and D. R. Smith, IEEE Antennas Propag. Mag. **54**, 10 (2012).
4. A. V. Kildishev, A. Boltasseva, and V. M. Shalaev, Science **339**, 1232009 (2013).
5. P. Genevet and F. Capasso, Reports on Prog. Phys. **78**, 024401 (2015).
6. J. Hu, S. Bandyopadhyay, Y.-h. Liu, and L.-y. Shao, Front. Phys. **8** (2021).
7. X. Zhao, Z. Sun, L. Zhang, Z. Wang, R. Xie, J. Zhao, R. You, and Z. You, Adv. Devices & Instrum. **2022** (2022).
8. V. S. Asadchy, M. S. Mirmoosa, A. Díaz-Rubio, S. Fan, and S. A. Tretyakov, Proc. IEEE **108**, 1684 (2020).
9. A. M. Mahmoud, A. R. Davoyan, and N. Engheta, Nat. Commun. **6**, 8359 (2015).
10. L. D. Bino, J. M. Silver, M. T. M. Woodley, S. L. Stebbings, X. Zhao, and P. Del'Haye, Optica **5**, 279 (2018).
11. D. L. Sounas, J. Soric, and A. Alú, Nat. Electron. **1**, 113 (2018).
12. S. S. Kruk, L. Wang, B. Sain, Z. Dong, J. Yang, T. Zentgraf, and Y. Kivshar, Nat. Photonics **16**, 561 (2022).
13. N. M. Litchinitser, Adv. Physics: X **3**, 1367628 (2018).
14. M. Ren, E. Plum, J. Xu, and N. I. Zheludev, Nat. Commun. **3**, 833 (2012).
15. M. Matuszewski, W. Krolikowski, and Y. S. Kivshar, Opt. Express **16**, 1371 (2008).
16. A. Valipour, M. H. Kargozarfard, M. Rakhshi, A. Yaghootian, and H. M. Sedighi, Proc. Inst. Mech. Eng. Part L: J. Materials: Des. Appl. **236**, 2171 (2022).
17. W. Zhang, Q. Song, W. Zhu, Z. Shen, P. Chong, D. P. Tsai, C. Qiu, and A. Q. Liu, Adv. Physics: X **3**, 1417055 (2018).
18. Y. A. Urzhumov, G. Shvets, J. Fan, F. Capasso, D. Brandl, and P. Nordlander, Opt. Express **15**, 14129 (2007).
19. A. A. Zharov, A. A. Zharov, and N. A. Zharova, J. Opt. Soc. Am. B **31**, 559 (2014).
20. M. Liu, K. Fan, W. Padilla, D. A. Powell, X. Zhang, and I. V. Shadrivov, Adv. Mater. **28**, 1553 (2016).
21. A. Zharov, Z. Viskadourakis, G. Kenanakis, V. Fierro, and A. Celzard, Nanomaterials **11** (2021).
22. A. Zharov, V. Fierro, and A. Celzard, J. Opt. Soc. Am. B **39**, 1307 (2022).
23. A. Zharov, V. Fierro, and A. Celzard, Phys. Rev. A **106**, 013504 (2022).
24. V. S. Asadchy, A. Díaz-Rubio, and S. A. Tretyakov, Nanophotonics **7**, 1069 (2018).
25. J. Hansen and I. McDonald, *Theory of Simple Liquids* (Elsevier Science, 2006).
26. https://refractiveindex.info/.
27. M. G. Blaber, M. D. Arnold, and M. J. Ford, The J. Phys. Chem. C **113**, 3041 (2009).
28. Y. Shi, Z. Yu, and S. Fan, Nat. Photonics **9**, 388 (2015).